The VSPA Foot: A Quasi-Passive Ankle-Foot Prosthesis With Continuously Variable Stiffness

Max K. Shepherd, *Student Member, IEEE*, and Elliott J. Rouse, *Member, IEEE*

***Abstract*— Most commercially available prosthetic feet do not exhibit a biomimetic torque-angle relationship, and are unable to modulate their mechanics to assist with other mobility tasks, such as stairs and ramps. In this paper, we present a quasi-passive ankle-foot prosthesis with a customizable torque-angle curve and an ability to quickly modulate ankle stiffness between tasks. The customizable torque-angle curve is obtained with a cam-based transmission and a fiberglass leaf spring. To achieve variable stiffness, the leaf spring's support conditions can be actively modulated by a small motor, shifting the torque-angle curve to be more or less stiff. We introduce the design, characterize the available torque-angle curves, and present kinematics from a transtibial amputee subject performing level-ground walking, stair ascent/descent, and ramp ascent/descent. The subject exhibited a more normative range of motion on stairs and ramps at lower stiffness levels, and preferred different stiffness levels for each task. Paired with an appropriate intent recognition system, our novel ankle prosthesis could improve gait biomechanics during walking and many other mobility tasks.**

***Index Terms*— Assistive technology, prosthetic limbs, quasi-passive, quasi-stiffness, variable-stiffness, prosthesis design.**

I. Introduction

THE majority of the 600,000 Americans living with a major lower limb amputation use passive ankle-foot prostheses, which behave much like a spring [1], [2]. The intent of these prostheses is to provide some energy storage, while being simple and anthropometric. However, due to limitations in current technology, transtibial amputees using passive prostheses experience a number of difficulties; self-selected walking speed is reduced, the metabolic cost of walking is higher, falls are more likely, and ambulation tasks, such as traversing stairs and ramps, become more difficult [3]–[5].

The most efficient passive prosthetic feet are typically constructed from carbon fiber, and store energy during the stance phase of gait. This energy is returned during ankle "push-off," to propel the amputee into their next step. However, there are several major limitations with these "Energy Storage and Return" (ESR) feet. First, ESR feet do not appropriately mimic the nonlinear shape of the torque-angle curve during the stance phase of gait. This may have several disadvantages, such as increased resistance to tibial progression and prolonged heel-only contact [2], [6], [7]. Second, the stiffness of ESR feet is often optimized for level-ground walking, but may be far from ideal during other mobility tasks, such as ascending and descending stairs and ramps, walking on uneven terrain, or quiet standing. For instance, standing balance may benefit from higher ankle stiffness [8], while ambulating over stairs and ramps may be easier with a lower stiffness and an increased range of motion [9], [10]. There are commercially available prosthetic ankle-feet that use complex configurations of carbon fiber springs to produce more comfortable stiffness and damping characteristics during level-ground walking, but modification to the mechanical properties is typically not possible after production.

To improve performance on ramps and stairs, quasi-passive ankles—which can vary the mechanical properties of the prosthesis, but cannot add any net-positive mechanical energy into the gait cycle—have recently been successfully commercialized, and may improve biomechanics during a range of tasks. Variable damping ankle-foot prostheses, which use a hydraulic unit to regulate damping (such as the *Elan Foot*, from Endolite, Miamisburg, OH, USA), may help adapt to uneven ground and improve biomechanics on ramps [11]. An alternative quasi-passive strategy is to modify the equilibrium angle for different activities. The *Proprio Foot* by Össur uses this strategy, and has shown benefit to users traversing stairs and ramps [12], [13]. These ankle-feet highlight the potential for quasi-passive designs that are a lightweight, robust, quiet, and inexpensive alternative to fully powered prostheses. However, despite encouraging work, there have been few studies focusing on the development of quasi-passive prostheses that can vary their stiffness properties, rather than damping or equilibrium position.

Manuscript received October 20, 2016; revised March 28, 2017 and June 27, 2017; accepted August 20, 2017. Date of publication September 7, 2017; date of current version November 29, 2017. *(Corresponding author: Elliott J. Rouse.)*

M. K. Shepherd is with the Department of Biomedical Engineering, Northwestern University, Evanston, IL 60208 USA, and also with the Neurobionics Lab, Shirley Ryan AbilityLab, Chicago, IL 60610 USA.

E. J. Rouse was with the Neurobionics Lab, Center for Bionic Medicine, Shirley Ryan AbilityLab, Departments of Physical Medicine and Rehabilitation, Biomedical Engineering, and Mechanical Engineering, Northwestern University, Evanston, IL 60208 USA. He is now with the Neurobionics Lab, Department of Mechanical Engineering, University of Michigan, Ann Arbor, MI 48109 USA (e-mail: ejrouse@umich.edu).

Digital Object Identifier 10.1109/TNSRE.2017.2750113

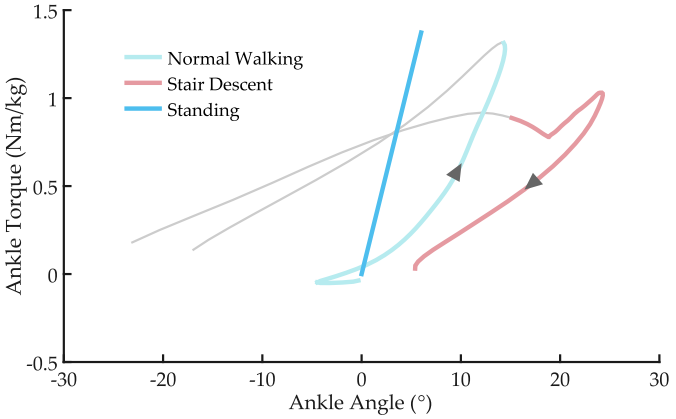

Fig. 1. Able-bodied ankle torque-angle curves for various tasks. Heel strike to push-off of normal walking and heel strike to toe-off of stair descent (from [15]) are shown with color, and estimated for a 70 kg subject. The gray portions illustrate push-off in level-ground walking and weight acceptance in stair descent, which cannot be accurately replicated with a quasi-passive prosthesis. An estimate of the equivalent stiffness of the ankle during quiet standing [26] is also shown.

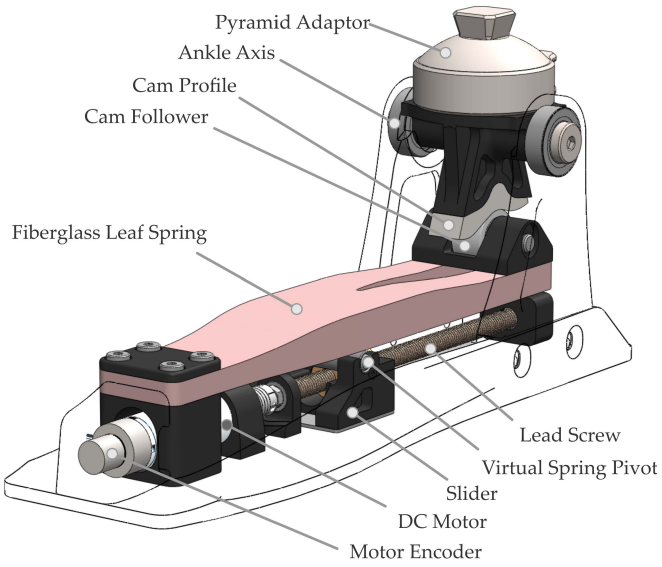

Fig. 2. Isometric view of the VSPA foot. The frame is displayed as transparent to show slider mechanism.

In this paper, we introduce the Variable-Stiffness Prosthetic Ankle-Foot (VSPA Foot). The VSPA Foot is a quasi-passive ankle-foot prosthesis with two key advantages and design innovations: 1) it has a nonlinear, custom torque-angle curve that can more accurately mimic biological ankle mechanics, and 2) it is able to perform online modulation of the overall stiffness for different mobility tasks. A cam-based transmission enables the custom, nonlinear torque-angle curve, and the stiffness is modulated by motorized reconfiguration of the spring support conditions. In this paper we introduce the VSPA Foot design, characterize its mechanical performance, and provide preliminary testing with a transtibial amputee performing various mobility tasks. Details of the design were also included in the proceedings of the 2017 International Conference on Robotics and Automation [14].

II. Background and Rationale

A. The Case for a Nonlinear, Customizable Torque-Angle Curve

A primary goal of this prosthesis is to be capable of producing a nonlinear torque-angle curve, which will enable optimal reproduction of the able-bodied torque-angle curve during level-ground walking. The kinetics and kinematics during level-ground walking were found for different speeds by Bovi *et al.* [15], and stance phase for self-selected walking speed is reproduced in Fig. 1.

A passive or quasi-passive prosthesis cannot perfectly replicate the full torque-angle curve, because the human ankle produces net-positive mechanical work during the gait cycle. The ideal torque-angle curve for a passive prosthesis is unknown, but we have focused on replicating the first two phases of the biological torque-angle curve, often referred to as "controlled plantarflexion" (i.e., heel-strike to foot-flat), and "controlled dorsiflexion" (i.e., progression of the body over the foot, until ankle push-off). There were three reasons to focus on this region of stance phase. First, Rouse *et al.* showed that the ankle's stiffness (a component of the joint impedance) closely resembles the quasi-stiffness during stance phase [16]. For a passive system, the quasi-stiffness and stiffness are equivalent concepts (for a thorough explanation of the difference, see [17]). Thus, by accurately following the concave-up shape of the torque-angle curve, we are also imitating the increasing joint impedance of an intact ankle, and potentially improving the dynamic response to perturbations from the environment.

Second, the relatively high stiffness of ESR feet in early stance likely inhibits tibial progression, something amputees often refer to as a "dead spot" that they have to "climb over" [6]. A custom nonlinear torque-angle curve could remove this dead spot with lower stiffness in early stance, while preserving the higher stiffness in late stance that promotes energy storage.

Third, significantly decreased stiffness during heel strike (controlled plantarflexion) is paramount to reducing the time of heel-only contact with the ground, and quickly achieving foot-flat for improved stability [2], [7], [18]. Many ESR feet use a shock-absorbing heel that simulates weight acceptance, but the high rotational stiffness does not appropriately lead to foot-flat. Amputees also show significantly decreased knee flexion in early stance (7° compared to 15°), indicating an inability for the knee to absorb the shock of impact [7].

There is some inconsistency in the literature in quantifying peak torques and magnitude of positive net work at the ankle during walking (compare [15], [19]–[21]). However, the low stiffness during heel strike and the increasing stiffness during stance phase is consistent. Inappropriate selection of ankle stiffness may have a multitude of detrimental side effects, including increased gait asymmetries, loss of stability, increased loading through the socket, and pain [2], [18]. While more research is needed to determine the ideal torque-angle curve for a passive (or quasi-passive) ankle, we believe it's

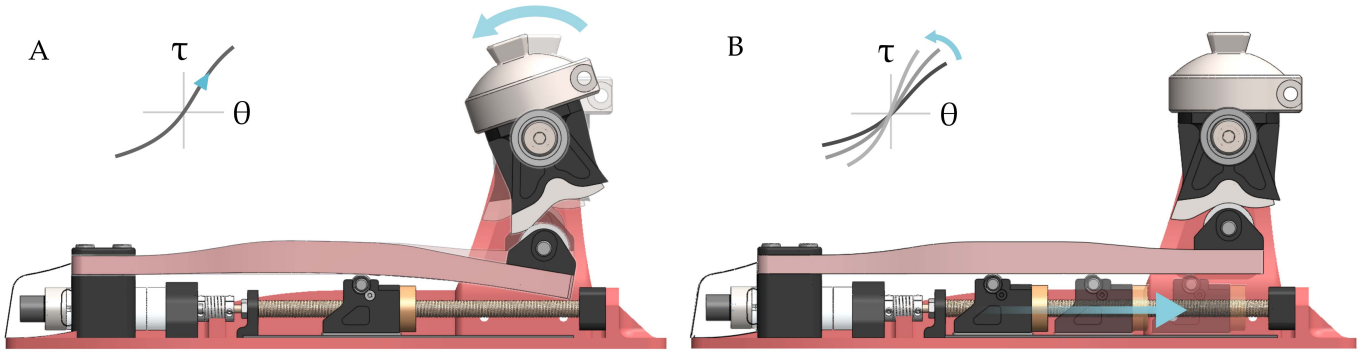

Fig. 3. (A) Rotation of the ankle joint causes downward deflection of the leaf spring, with the cam follower being displaced by the cam profile. This enables a nonlinear, customizable torque-angle curve. The cam profile is designed to produce the "primary torque-angle curve" when the slider is in the "primary slider position." (B) The motor can move the simple support ("slider") via a lead screw, modifying the stiffness of the leaf spring. This shifts the mechanics away from the primary torque-angle-curve, to be more or less stiff overall.

likely nonlinear, and the ability for customization is important for avoiding these challenges.

B. The Case for Different Stiffness Levels During Stairs, Ramps, and Standing

There are major kinematic differences between ESR feet and intact human ankles. In particular, during both stair ascent and descent, the high stiffness of the prosthesis hinders progression of the center of mass over the prosthesis [10]. This results in slower gait speeds, compensatory gait patterns, and more muscular effort required [9]. In particular, during stair descent, the intact ankle typically exhibits large dorsiflexion displacements, up to 23° , to allow forward progression and lowering of the center of mass. By comparison, the Seattle LightFoot (Trulife, Dublin, IRL) only yields 10° [9]. Able-bodied subjects exhibit a lower quasi-stiffness during the controlled dorsiflexion phase of stair descent than for level-ground walking (Fig. 1) [15]. By decreasing stiffness below the ideal stiffness for level-ground walking, we may see more normative range of motion, and amputees may reduce compensatory patterns they have developed in response to the reduced range of motion.

Limited range of motion due to high stiffness has also been suggested as a key factor in creating instability when unilateral transtibial amputees walk on un-level ground, such as ramps [11], [22]. The *Proprio-Foot* attempts to solve this problem by changing the equilibrium angle of the foot, as have several research devices [12], [23], [24]. Alternatively, decreasing the stiffness may allow an increased range of motion, with the heel reaching foot-flat more quickly, and the tibia progressing easily during mid-stance.

Finally, transtibial amputees have impaired standing balance, as indicated by increased anteroposterior sway and lateral weight distribution [25]. Using an inverted pendulum model, Morasso and Schieppati [26] found an equivalent passive stiffness per ankle may be approximately 16 Nm/degree (see Fig. 1) for a 70 kg subject. Similarly, a study of effective roll-over shapes with able-bodied subjects found that the equivalent prosthesis stiffness would need to be about three times higher for standing than for walking [8].

III. Design

A. Mechanical Description

The VSPA Foot (Fig. 2) combines two key design elements: a cam-based transmission enabling a customizable torque-angle curve (Fig. 3a), and a variable stiffness leaf spring (Fig. 3b). When the ankle rotates, the cam profile is in contact with the cam follower, which deflects the leaf spring. The deflection of the leaf spring stores energy, and provides a restoring torque on the ankle joint. By appropriately designing the shape of the cam profile, the torque-angle curve at the ankle can take any desired shape—not necessarily linear. The stiffness of the leaf spring can also be varied (when unloaded) by actively moving the simple support ("slider") with an electric motor. Changing the stiffness of the leaf spring alters the torque-angle curve at the ankle, making it more or less stiff overall. We believe the biomechanics of level-ground walking are the most important to provide accurately, thus the cam profile presented in this work is designed to reproduce the early and mid-stance torque-angle curve for walking—and from this desired torque-angle curve, we can modulate the ankle mechanics to be more or less stiff for various ambulation modes. We define this governing curve the "primary torque-angle curve, " and it occurs at the "primary slider position." It should be noted that moving the slider changes the overall stiffness, but the shapes of the available torque-angle curves are defined by the cam profile.

1) Cam-Based Transmission: Rotation of the ankle joint creates a downward deflection of the free end of the leaf spring, through a rolling cam transmission. The deflected leaf spring in turn creates a restoring torque at the ankle joint. The cam profile governs the torque-angle curve at the ankle; with the appropriate description of this relationship, a cam profile can be created for virtually any arbitrary desired torque-angle curve (see the following section).

The cam profile is machined from tool steel, and hardened to approximately 60 Rockwell C, to avoid plastic deformation at high loads. The 19 mm cam follower (Misumi USA, Schaumburg IL) is designed for dynamic loads up to 7.6 kN. The leaf spring is constructed from unidirectional

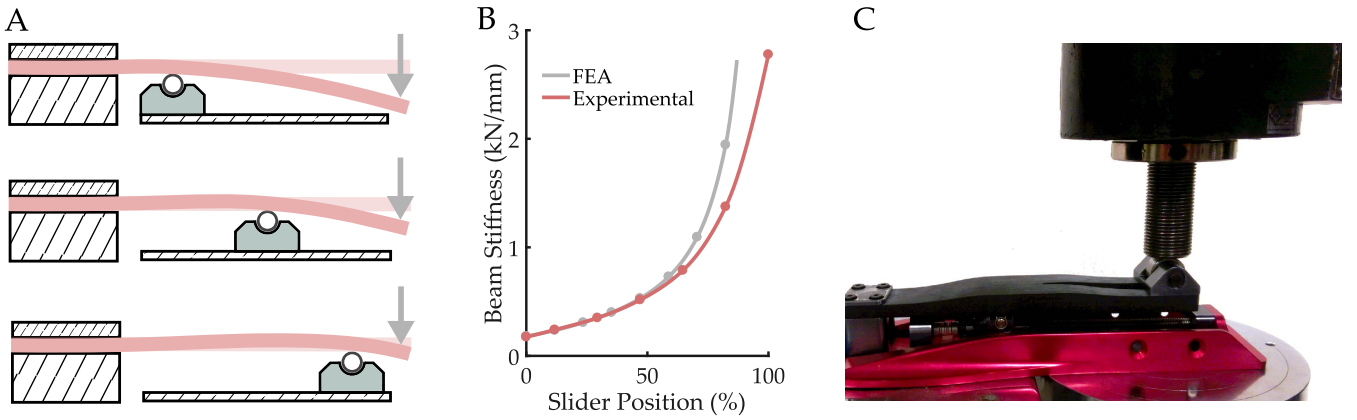

Fig. 4. (A) Illustration of how the support conditions affect the leaf spring stiffness. As the slider moves towards the load, the stiffness increases. (B) Experimental and FEA simulation results for translational spring stiffness as a function of slider position. The points are tested slider positions. (C) Testing apparatus. The load cell (top right) is lowered onto the cam follower (with the cam profile, ankle joint, and upright supports removed).

fiberglass (E-glass), and custom machined (Gordon Composites, CO, USA). Fiberglass was chosen for the spring material because of its excellent energy-storage capacity per weight—up to 8 times higher than spring steel [27]. A small preload is added to the spring to reduce backlash that may be induced by hysteresis in the fiberglass.

2) Torque-Angle/Stiffness Modulation: The ankle's torque-angle curve can be altered by repositioning the slider beneath the fiberglass leaf spring. By supporting the spring closer to the load, the translational stiffness of the spring increases (Fig. 4a). This concept has been used in variable stiffness actuators, as well as an ankle prosthesis that changes stiffness in the frontal plane for improved terrain negotiation [28], [29].

The fiberglass spring was designed with varying spring height in order to maintain relatively consistent ultimate strength along the outer strands, and appropriate strength across the range of slider positions. This was accomplished through iterative Finite Element Analysis (FEA) in Solidworks (Dassault Systèmes, Vélizy-Villacoublay, FRA). At lower stiffness levels, hard mechanical stops (which prevent the ankle from rotating past 30° of dorsiflexion or plantarflexion) are engaged before the spring would fracture; at higher ankle stiffness levels, the spring strength limits the maximum deflection and torque (Fig. 5).

The spring was also designed with iterative FEA to have an appropriate range of translational stiffness levels available (Fig. 4b). An elastic modulus of 24.5 GPa was used, which we have found to accurately describe experimental characterizations of other fiberglass springs from this manufacturer. To more accurately predict the range of torque-angle curves that will be available at the ankle joint, and to inform the specified location of the primary slider position, the translational stiffness of the leaf spring was experimentally measured using a materials testing system (Sintech 20g, MTS, Eden Prairie, MN). The loads were applied directly to the cam follower (Fig. 4c) at different slider positions. Across the slider's range of motion, over an order of magnitude of translational stiffness values are available (Fig. 4b), with similar stiffness trends predicted by the FEA.

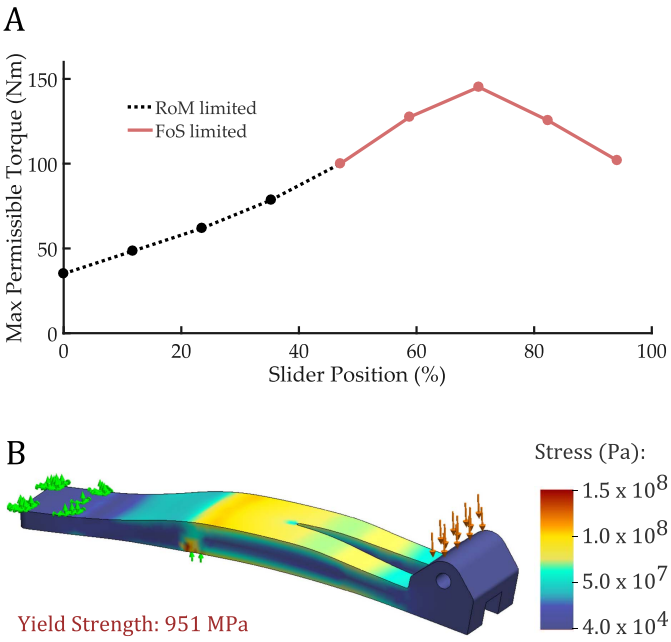

Fig. 5. (A) The maximum permissible torque for the chosen cam profile depends on slider position, and is limited by either ankle Range of Motion (RoM), with hard stops at $\theta = \pm 30°$, or spring strength (shown is an estimate of the max. torque with a Factor of Safety of 2.) (B) The spring strength was estimated using FEA at different slider positions.

The slider is repositioned by a 10 W DC motor with a 3.9:1 planetary gearhead (DCX 16 L, Maxon Motors, CHE), which drives a 6.35 mm diameter leadscrew with a 1.27 mm lead (Nook Industries, OH, USA). The lead screw is supported by angular contact bearings (New Hampshire Ball Bearings, Peterborough, NH; model SSMER-2SD503.) To minimize size and weight of the slider, no rails or bearings were used; instead, the sliding interface with the chassis comprises two 1 mm thick Delrin pads, and the interface between slider and leaf spring is a freely rotating shaft supported by PTFE-lined bronze/steel bushings. The lead screw is nonbackdrivable; thus, the motor is not required to provide a holding torque when the spring is loaded. Modulation of stiffness is not

TABLE I
MASS OF COMPONENTS

Component	Mass (g)
Spring	107
Lead screw	28
Battery	61
Electronics + box (not including battery)	109
Motor + gearhead + encoder	72
Slider	38
Cam profile	25
Pyramid adapter	65
Aluminum frame	315
Other machined components	129
Other hardware	129
Total	**1078**

possible when the spring is loaded. The ankle must be at 0°, its equilibrium angle, to reposition the slider.

The motor is controlled by an EPOS2 positioning controller (Maxon Motors) which uses the incremental motor encoder (1024 counts per revolution) for position sensing. A single board computer (Raspberry Pi Zero, Raspberry Pi Foundation, Cambridgeshire, UK) sends step/direction commands to the motor controller, which scales individual steps to 1 mm of slider movement. The single board computer also acquires ankle angle from a 14-bit contactless encoder placed on the ankle axis (AS5048A AMS, Premstaetten, AUT) over SPI. A 14.8 V LiPo battery (Venom, Rashdrum, ID, USA) powers the electronics. All electronics are housed onboard in a custom electronics enclosure, which can be mounted to the prosthesis socket.

The frame is constructed from machined and anodized 7075-T6 aluminum. The prosthesis can be attached to an amputee's socket via a standard titanium pyramid adaptor (Bulldog Tools, Lewisburg, Ohio USA), which also allows internal/external rotation adjustment. The ankle, including electronics, weighs 1.1 kg (for the mass of individual components, see Table I.) For comparison, the commercial variable-damping *Elan Foot* is advertised as weighing 1.2 kg, and the fully powered *BiOM* ankle-foot (Bionx Medical Technologies) weighs 2.3 kg.

B. Cam Design

The torque-angle curve is governed by the stiffness of the leaf spring and the shape of the cam profile. Although the mechanics of the ankle can be varied from the primary torque-angle curve, the primary torque-angle curve itself cannot be changed following manufacturing, since the cam profile is a custom machined part. The purpose of this section is to provide the mathematical instructions to convert a desired primary torque-angle curve at a desired slider position to the corresponding cam profile.

A diagram of the system and variables is shown in Fig. 6. The cam follower is modeled as a point; the final curve will have an offset equal to the cam follower radius. The leaf spring is modeled as a rotary spring, because (1) the follower does not travel vertically when the spring is deflected, and (2) non-vertical forces on the follower generate a moment on the spring, because the point of force application is above the neutral plane of the spring. The spring thus rotates about a "virtual pivot," which we approximate as the location of the simple support. The true location of the virtual pivot is likely closer to the cam and polycentric, but the mathematics are insensitive to small errors in this parameter. A more precise calculation of this virtual pivot may be found using pseudo-rigid-body modeling [30].

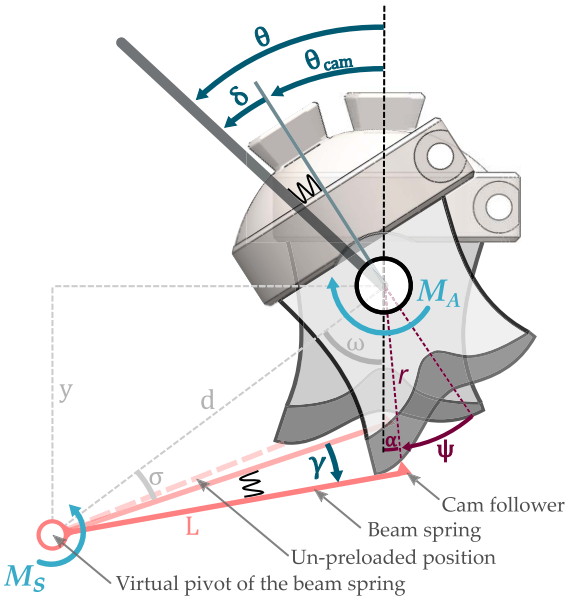

Fig. 6. The work stored at the ankle joint is equal to the work stored in the leaf spring (modeled as a rotational spring with a virtual pivot). The cam follower is simplified to a point (indicated by the pink triangle.) Downward deflection of the cam follower γ creates a restoring moment in the leaf spring (M_S). Deflection of the ankle θ is a combination of the cam deflection (θ_{cam}) and series compliance (δ); it causes a moment at the ankle (M_A), produced by the force between the cam follower and cam profile. The leaf spring is preloaded a small angle. Shown in gray is geometry used to solve for cam radius (r) from γ, and ψ from θ. The final cam profile is solved in polar coordinates (r, ψ). Note, the profile would still require an offset for the final curve to work with the actual cam follower (the shown curve is without offset for illustration purposes.).

Early experiments with our preliminary cam profile indicated series compliance due to flexure of the aluminum prosthesis frame, which had unwanted effects on the ankle's torque-angle curve. To add this series compliance into our mathematical model, we assume the unwanted deflection δ is proportional to the ankle moment (with experimentally determined stiffness of approximately 1200 Nm/rad), and acts between the cam and user.

Rather than utilizing a statics-based approach to solve for the cam profile [31], which quickly becomes intractable with a sophisticated geometry and series compliance, we instead frame the problem using the principle of virtual work. That is, assuming no energy loss in the transmission or spring, the energy stored in the ankle (minus energy stored in the series compliance) is equal to the energy stored in the leaf spring:

$$\int_0^{\gamma} M_S d\gamma = \int_0^{\theta} M_A d\theta - \int_0^{\delta} M_A d\delta \tag{1}$$

where γ is the angular deflection of the rotary spring, M_S is the spring moment, θ is the ankle angle, δ is the series frame compliance, and M_A is the ankle torque (Fig. 6). The right side of this equation is known as a function of θ—we are specifying the desired torque-angle curve at the ankle, and can thus simply numerically integrate both the desired torque-angle curve and the known series compliance. For simplicity, we solve dorsiflexion and plantarflexion individually, so the lower limit of integration is 0. At the equilibrium position $\theta = 0°$, the spring is preloaded a small angle γ_0. Equation 1 can be written as

$$\int_0^{\gamma} k(\gamma + \gamma_0)d\gamma = \int_0^{\theta} M_A d\theta - \int_0^{\delta} M_A d\delta \tag{2}$$

where k is the rotational stiffness of the leaf spring, converted from the experimental results for the translational stiffness (Fig. 4b). The left side of this equation may be integrated to

$$\frac{1}{2}k\gamma^2 + k\gamma_0\gamma + c = \int_0^{\theta} M_A d\theta - \int_0^{\delta} M_A d\delta \tag{3}$$

where the constant of integration, c, can be found to be zero from the initial conditions: $\theta = 0, \gamma = 0$. We then use the quadratic formula to solve for γ as a function of θ:

$$\gamma(\theta) = -\gamma_0 + \sqrt{\gamma_0^2 + \frac{2}{k}\left(\int_0^{\theta} M_A d\theta - \int_0^{\delta} M_A d\delta\right)}. \tag{4}$$

We now have γ, the leaf spring angle, as a function of the ankle angle θ (both integrals can be evaluated numerically.) We can derive the radius r of the cam profile as a function of θ, from γ and the defined geometry (via law of cosines):

$$r(\theta) = \sqrt{L^2 + d^2 - 2Ld\cos(\gamma + \sigma)}. \tag{5}$$

Finally, to have a polar representation (r, ψ) of the cam profile in the cam reference frame, we need ψ as a function of θ:

$$\psi(\theta) = \theta_{cam} - \alpha = \theta - \delta - \alpha. \tag{6}$$

We can find α (the small deviation from vertical) using the law of sines:

$$\alpha(\theta) = sin^{-1}(L\sin(\sigma + \gamma(\theta))) + \omega. \tag{7}$$

The numerical results are now in polar coordinates as (r, ψ). This curve is converted to Cartesian coordinates, and a parallel curve corresponding to the final cam profile is created with a perpendicular offset equal to the cam follower radius.

An inverse model was also created, which determined the torque-angle curve at the ankle for a given cam profile and slider position. Slider repositioning was simulated by adjusting the preload γ_0, rotational stiffness k, and the geometric parameters d and σ describing the position of the virtual pivot relative to the ankle axis. An overview of the modeling and characterization process is shown in Fig. 7.

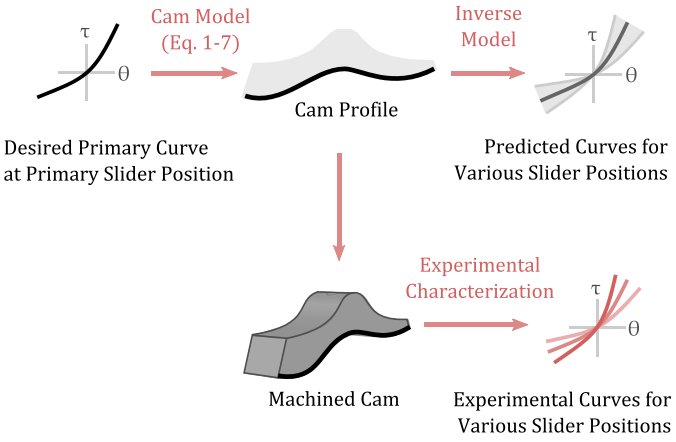

Fig. 7. The presented mathematics (Eq. 1–7) describe the derivation of a cam profile from a desired primary torque-angle curve and a primary slider position. This cam profile is machined, and the torque-angle curves of the VSPA Foot are experimentally determined for various slider positions. An inverse model was also created to predict the range of curves that would be available.

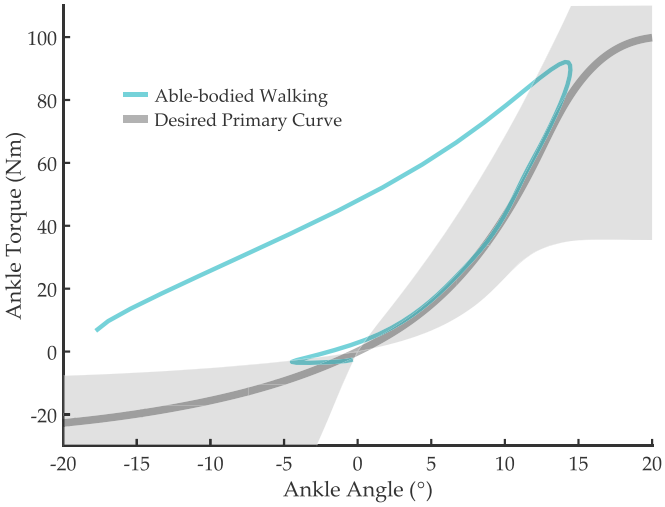

Fig. 8. Desired primary torque-angle curve for walking (gray), with other stiffness levels predicted for the range of slider positions. The able-bodied torque-angle curve [15] is shown in blue for a 70 kg subject. Positive angle indicates dorsiflexion, and positive torque is in plantarflexion.

C. Desired Primary Torque-Angle Curve

For our pilot testing, we chose to design a cam that would produce the nonlinear torque-angle curve shown in Fig. 8. With this curve, we hoped to provide appropriate compliance in controlled plantarflexion, and closely follow the shape of the able-bodied torque angle curve during controlled dorsiflexion, for the reasons mentioned in Section II. The curve must have zero torque at $\theta = 0°$, so that a bias torque isn't present during standing, and to allow appropriate foot clearance during swing phase. Naturally, like other passive or quasi-passive prostheses, we are unable to mimic powered plantarflexion.

The primary slider position was chosen to be at 47% of its range of motion, to allow an appropriate range of more stiff and less stiff torque-angle curves. The desired primary torque-angle curve we have selected for this pilot study is shown in Fig. 8. Also shown in Fig. 8 is the predicted

range of torque-angle curves available with the corresponding cam profile at different slider positions. At large dorsiflexion angles, the torque becomes constant; this reduces the load on the spring at high deflections, and creates an appropriately sized cam such that the spring doesn't interfere with the lead screw before the hard stops are reached. As described previously, the desired curve was created to smoothly approximate the torque-angle curve from Bovi *et al.* [15] during controlled plantarflexion and controlled dorsiflexion. The curve was created with a cubic spline interpolation of the points $\theta = [-0.65, -0.5, -0.2, 0, 0.125, 0.21, 0.24, 0.4, 0.5, 0.65]$, $\tau = [-25, -25, -17, 0, 25, 60, 76, 100, 100, 100]$. It should be noted that, while we have provided biologically-motivated rationale for the specific curve we have chosen for initial testing, the ideal torque-angle curve is unknown. Future work is still needed to determine the true effects of this curve on gait biomechanics.

IV. Experimental Methods

A. Characterization of VSPA Foot Mechanics

For simplicity, slider positions will be identified relative to the primary slider position (e.g., $x = -20$ mm refers to a slider position 20 mm closer to the forefoot than the primary slider position, and is less stiff than the primary torque-angle curve).

The desired primary torque-angle curve (the input to our model) and torque-angle curves possible across the slider range were experimentally determined using the Neurobionics Lab Rotary Dynamometer, a custom dynamometer consisting of a frame-mounted motor (BSM90N-3150AF, Baldor, Fort Smith, AR) and 6-axis load cell on the motor output (45E15A M63J, JR3, Inc., Woodland, CA, USA), sampling torque at 1 kHz. The prosthesis's pyramid adapter was rigidly secured to the machine, and the ankle was aligned with the dynamometer's rotational axis with a concentric laser. Ankle angle was measured using the onboard ankle angle encoder at approximately 100 Hz. The torque-angle curve was determined at different slider positions, in both plantar and dorsiflexion separately. As the stiffness increased, the range of motion tested was decreased, so as not to overload any components of the ankle.

The speed of stiffness transition was tested offline with the ankle at the neutral position. The desired slider position was instantaneously changed from standing stiffness ($x = 45$ mm) to walking stiffness ($x = 0$ mm) and other stiffness levels. The motor angle was measured with the motor encoder, and recorded using the EPOS Studio software (Maxon Motors). The actual slider position was calculated from the motor angle using the transmission ratio.

B. Clinical Testing

One transtibial amputee (age: 40, height: 1.55 m, weight: 75 kg, time since amputation: 3 years, home prosthesis: *Senator Foot,* an ESR foot by Freedom Innovations) was recruited to perform different mobility tasks with the VSPA Foot. This portion of the study was approved by the Northwestern University Institutional Review Board, and informed written consent was obtained from the subject. The VSPA Foot was fixed to the subject's socket, and aligned by a certified prosthetist. The electronics enclosure was mounted to the socket with self-adherent wrap, and communicated wirelessly with a laptop. The VSPA Foot was used with an athletic shoe to provide a more realistic testing condition.

For the level-ground walking trials, the subject walked on a treadmill at a self-selected speed, which was permitted to vary between trials. Walking speed was permitted to vary because the subject indicated discomfort upon attempting a consistent walking speed across lower stiffness levels. Once the subject indicated feeling comfortable at the selected speed, ankle angle was recorded for 60 s. The subject occasionally rested in between trials. Five stiffness levels were tested: $x = -20$ mm, -10 mm, 0 mm, 10 mm and 20 mm. Following the trials at each of the five stiffness levels, the slider position was adjusted based on subject preference. These adjustments were made in small increments during the swing phase of gait; the subject did not stop walking during this portion of the experiment. After each adjustment, the subject walked several steps and then indicated whether they preferred it more or less than the previous stiffness, or did not have a preference. Torque data were obtained using kinematics and known torque-angle characterization.

For stair ascent and descent, the subject ambulated over a 4-step staircase, prosthesis side first, and was permitted to use the hand rails. For ramp ascent and descent, the subject walked up and down a 4.4 m long ramp of 11° incline, and was permitted to use the hand rails. For both ramp and stair tests, the subject walked up, turned around, paused briefly, and then descended. Five stiffness levels were tested: $x = -30$ mm, -20 mm, -10 mm, 0 mm and 10 mm. Three trials were performed at each stiffness level; the first was considered a practice, and the second and third trials were included in the data analysis. Between trials of ramp descent and stair descent, the subject was asked to comment on their preferred ankle-foot stiffness. Torque data were obtained using kinematics and known torque-angle characterization, but are not presented.

Slider position and ankle angle were recorded at 100 Hz for all trials. Ankle angle is bidirectionally (zero-lag) filtered with a 6 Hz, 4^{th} order Butterworth filter. All trials for walking, stair descent, and ramp ascent/descent are aligned by peak dorsiflexion, because it is a consistently identifiable gait event, and to highlight the effect stiffness has on dorsiflexion range of motion.

V. Results

A. VSPA Foot Characterization

The ankle torque-angle curves at several slider positions are shown in Fig. 9. The desired primary torque-angle curve is shown in gray, and the experimentally determined torque-angle curve at the primary slider position is shown dashed in pink. The fidelity of the experimental results validates the mathematical methods that constructed the cam profile.

The stiffness around $\theta = 0°$ can be varied by an order of magnitude at small angles; calculated as the average stiffness between -1° and 1°, stiffness around $\theta = 0°$ is 9.2 Nm/deg for

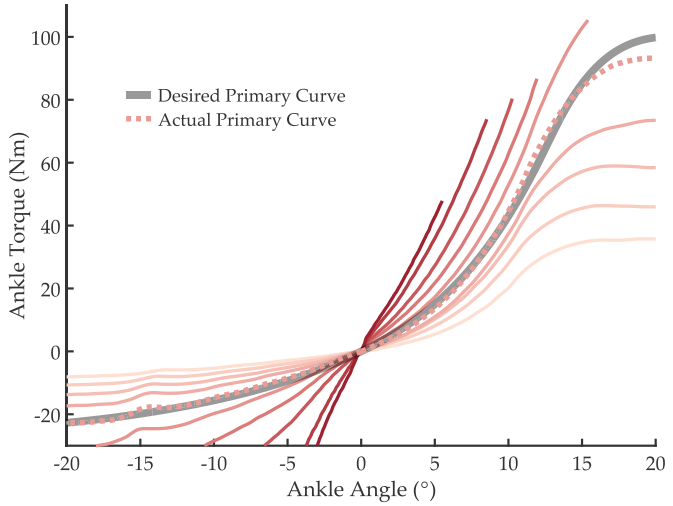

Fig. 9. Experimental characterization of the torque-angle curves possible across the range of slider positions. The desired primary torque-angle curve is shown in gray (dashed), and the experimentally-determined torque-angle curve at the primary slider position is shown dashed in color. All curves shown are during loading. The tested slider positions are, relative to the primary slider position, $x = -40$ mm, -30 mm, -20 mm, -10 mm, 0 mm, 10 mm, 20 mm, 30 mm, 40 mm, 45 mm. All ten curves are shown, with the lightest curve corresponding to x $= -40$ mm, and the darkest curve corresponding to $x = 45$ mm.

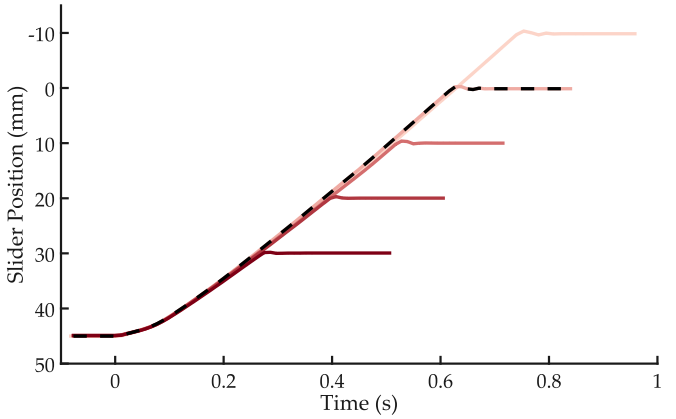

Fig. 10. Step responses from the highest stiffness to various slider positions. The dashed black line indicates a step to the primary slider position.

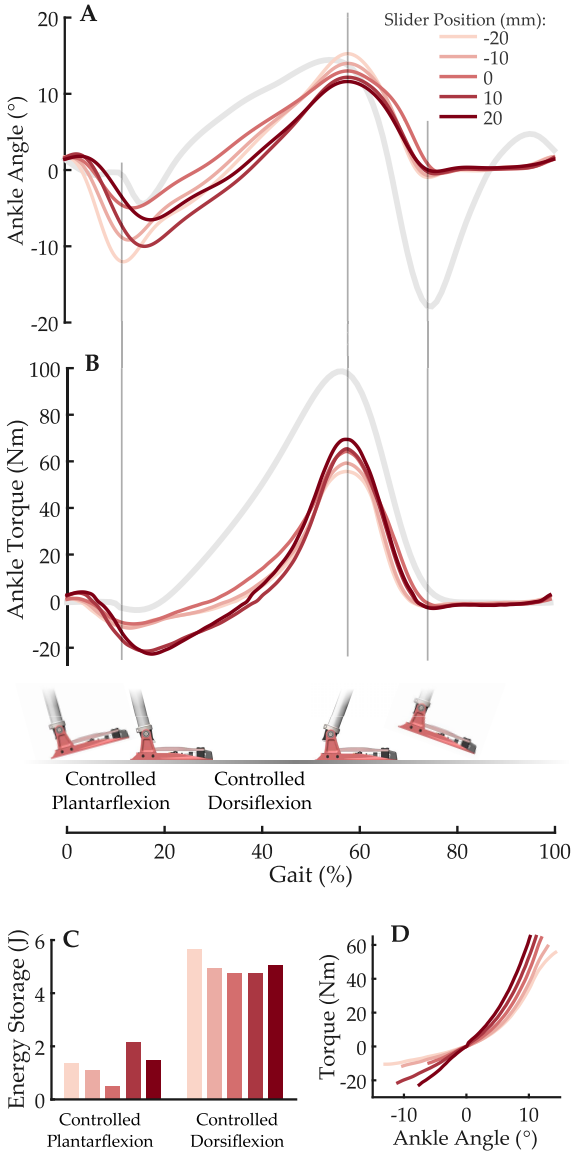

Fig. 11. Data from an amputee subject walking on a treadmill with the VSPA Foot at five stiffness levels. Walking data at each stiffness level is averaged from 37 steps sampled from one minute of continuous walking. Individual trials are aligned by peak plantarflexion, to avoid lowering of the mean peak dorsiflexion due to variability in the timing. Average gait cycles are also aligned by peak dorsiflexion, to highlight the effects of stiffness on range of motion and peak push-off torque. Able-bodied kinematics and kinetics from [15] are shown in gray (corrected for our subject's weight), with the gait cycle also aligned by peak torque (as opposed to heel strike). Vertical lines denote (from left to right) foot flat, heel off, toe off. Importantly, at lower stiffness levels, the subject requested slower treadmill speeds for comfort; stride period increased with stiffness: 1.49, 1.45, 1.45, 1.42, and 1.40 s. A) Prosthetic ankle range of motion during controlled dorsiflexion decreased at higher stiffness levels. B) Peak ankle torque increased at higher stiffness levels. Torque was derived from the experimental characterization of the ankle torque-angle curve at different slider positions. C) Energy stored by the prosthesis during controlled plantarflexion (heel strike to foot-flat) did not show a trend, but during controlled plantarflexion was increased at low stiffness. D) The mean torque-angle curves during walking, measured with the ankle encoder.

the stiffest torque-angle curve, and 0.68 Nm/deg at the least stiff curve. Hysteresis resulted in a loss of only 1.9% of the energy stored, averaging across all dorsiflexion trials.

Step responses of the slider repositioning are shown in Fig. 10. The speed is limited by mechanical constraints on the motor bearings and gearhead. Transitions from the highest stiffness to the primary slider position may be too slow to occur during one swing phase, but it is likely quick enough to allow smaller levels of repositioning for ramps and stairs.

B. Clinical Testing With an Amputee Subject

Results from the walking trials are shown in Fig. 11. The peak dorsiflexion during walking decreased at stiffer torque-angle curves, but the peak torque increased. Peak plantarflexion immediately following heel strike did not consistently decrease for this subject; at slider positions $x = 10$ mm and 20 mm, the peak plantarflexion increased, and the relative timing between foot-flat and push off was altered. This could be partially due to different walking speeds and stride frequency; at lower stiffness levels, the subject requested lower

treadmill speed due to discomfort, and stride period decreased consistently (at slider positions $x = -20$ mm, -10 mm, 0 mm, 10 mm, 20 mm, stride period was respectively 1.49 s, 1.45 s, 1.45 s, 1.42 s, 1.40 s). Walking speeds varied between 0.54 m/s and 0.85 m/s. The torque-angle curves at each stiffness level and the energy stored in plantarflexion and dorsiflexion are also shown in Fig. 11. Compliance in the shoe may contribute to lowering the overall stiffness.

For level-ground walking, the subject preferred a greater stiffness level than predicted. The subject indicated a preference for walking within the range of torque-angle curves corresponding to slider positions $x = 10$ mm through $x = 20$ mm. Adjustments of up to 5 mm within this range were not easily perceived by the subject. At low stiffness values, the ankle exhibited a small vibration following toe-off, behaving as an underdamped spring-mass system, but this response was minimal, and filtered out in post-processing.

During stair descent, the range of motion similarly increased at lower stiffness levels, indicating easier tibial progression (Fig. 12). Ground contact on the prosthesis side was made with the foot parallel to the ground, in contrast to able-bodied subjects who plantarflex before ground contact with their forefoot to absorb shock. The subject indicated a strong preference for the torque-angle curve corresponding to the slider position $x = -20$ mm. At the lowest stiffness, the increased range of motion delayed energy return, which the subject found uncomfortable.

Ramp ascent and descent at lower stiffness similarly elicited substantial and consistent increases in the range of motion during both controlled plantarflexion and dorsiflexion. In particular, at lower stiffness, ankle kinematics during ramp descent were more comparable to able-bodied kinematics on a 10° ramp reported in the literature [32]. The unusually high range of motion during controlled plantarflexion following heel strike indicates that the desired primary torque-angle curve may benefit from higher stiffness in this region. During ramp descent, the subject indicated a preference for the torque-angle curve corresponding to the slider position $x = -10$ mm. The kinematics for stair ascent and ramp ascent highly differ from able-bodied; these tasks may not be easily mimicked by a spring, as they involve large dorsiflexion during swing for toe clearance, and substantial powered push-off.

VI. Discussion

In this paper, we described the design, characterization, and validation of the VSPA Foot, a quasi-passive prosthetic ankle capable of a custom nonlinear torque-angle curve and adjustable stiffness. The characterization indicated that the ankle's torque-angle curve closely matched what was predicted from the mathematical model, and a substantial range of stiffness modulation is possible. The clinical test validated the performance of the ankle, and provided strong support for the potential advantages of stiffness modulation. As expected, range of motion increased at lower stiffness levels during walking on level ground, stairs, and ramps. In prior work, an increased range of motion on stairs and ramps has been suggested to improve gait [10], but without further biomechanical testing, the full effects and optimal stiffness during locomotion remain unknown. The largest improvement in kinematics was seen in stair descent, where the preferred stiffness involved a dramatic increase in range of motion. The peak dorsiflexion at

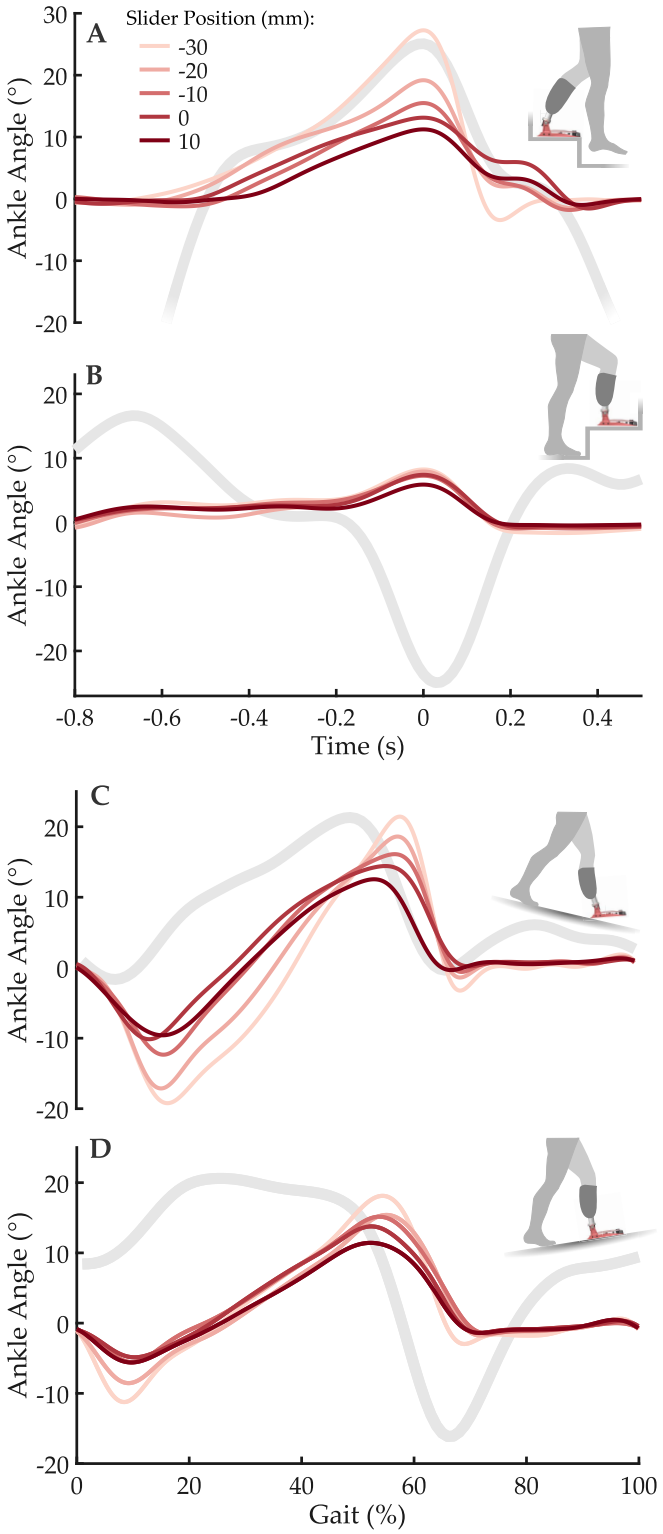

Fig. 12. Average prosthetic ankle kinematics for an amputee subject during A) stair descent, B) stair ascent, C) ramp descent, and D) ramp ascent. Also shown in gray are able-bodied kinematics (with stairs from [42] and ramps from [32]). Positive angles represent dorsiflexion. Decreasing ankle stiffness consistently increased range of dorsiflexion for all four tasks. For stair descent, the individual steps are aligned by peak dorsiflexion, to highlight the effect of stiffness on range of motion.

the preferred stiffness ($x = -20$ mm) was 19° —much closer to the dorsiflexion angles during able-bodied stair descent than traditional ESR feet obtain [9]. Perhaps among the most promising results is that the subject qualitatively preferred a different stiffness for each mobility task tested, despite limited practice. This preference provides an initial confirmation that the option of varying stiffness levels for different tasks may be beneficial. The range of preferred stiffness levels for the few mobility tasks tested varied by a factor of two (measured for small angles, varying from $x = -20$ mm during stair descent to around $x = 20$ mm during level-ground walking). However, reduction of stiffness past the preferred level for each task was particularly uncomfortable for the subject, indicating that stiffness would likely need to be tuned on a subject-specific basis.

The subject's desired stiffness during walking was higher than predicted; this may be because of higher similarity to the subject's prescribed prosthesis, or an indication that the ideal torque-angle curve is stiffer than would be motivated by able-bodied torque-angle curves. For level-ground walking, unlike stairs and ramps, we would not consider changes in range of motion to be a positive or negative indication; increased range of motion and increased energy storage during level-ground walking is not necessarily beneficial to the metabolic cost of walking [33]. We have provided rationale for the chosen shape of the primary torque-angle curve, but optimization would require a separate study looking at the broader effects of changes to this shape on gait biomechanics. The VSPA Foot also offers a simple and controlled platform for this experimentation.

To seamlessly modulate stiffness while transitioning between mobility tasks, the design presented here should be coupled with an intent recognition system. Intent recognition systems for lower limb prostheses have improved in recent years; experiments with a powered knee and ankle prostheses recently achieved transition and steady-state classification error rates of less than 1% using only onboard mechanical sensors (such as a six-axis load cell and inertial measurement unit) [34]. It's likely that intent recognition systems could be more accurate with transtibial amputees, because of the additional information from the intact knee.

A cam-based energy storage mechanism has been used in research to minimize the power requirements of a parallel actuator in an ankle prosthesis [31]. However, we believe the true advantage of a cam-based transmission in an ankle design is in its ability to simply, inexpensively, and robustly replace much of the function of a high-power motor, albeit without positive power push-off. A fully powered ankle could emulate the functions of this ankle, and more accurately mimic the positive net work performed by the biological ankle during gait. It is unclear, however, if powered ankles have a measurable advantage, such as improved metabolic cost [35], [36], or balance [37]. By removing a high power motor, large reduction transmission, and large battery, we can reduce weight, size, and complexity.

The rationale for this design is largely motivated by improving the mobility of unilateral transtibial amputees. However, we believe the VSPA Foot may also solve critical problems faced by bilateral amputees, transfemoral amputees, or amputees with comorbidities, such as diabetes. Bilateral amputees are unable to modulate their center of pressure via ankle control, so ankle-foot prostheses must be stiff enough to ensure standing stability. Su et al. suggested that less stiff prostheses with greater dorsiflexion may improve bilateral amputee gait, but may also decrease standing stability [38]. A prosthesis that can quickly adjust stiffness may ensure both standing stability and more normative gait. Vascular transtibial amputees have inferior standing balance control compared to trauma amputees, likely due to poor somatosensation [39]–[41]. Improvement of standing balance may be a higher priority for these patients.

Future designs of the VSPA Foot could address limitations in the current system. For example, with the slider in the stiffest position, the spring may not be strong enough for the user to walk (as could be the case if the supervisory intent recognition system mistakes walking for standing. See Fig. 5). This issue may best be addressed by limiting how close the slider gets to the cam follower, and using a stiffer leaf spring. The step responses with the slider also indicated that the speed of stiffness modulation may be too slow for certain activity transitions (Fig. 10). The speed could be improved with a more powerful motor or a better understanding of the force required to move the slider, allowing us to optimize the transmission ratio. Finally, the stiff forefoot may poorly approximate foot biomechanics during walking, in which the metatarsophalangeal joints extend to allow the heel to rise while the toes remain on the ground during late stance phase. If the prosthesis is shortened, a compliant feature could be added to the forefoot to better approximate this behavior.

Further work will also be needed to determine the ideal torque-angle curve for level-ground walking, as well as the range of stiffness levels necessary. In addition to potential commercialization, the device could be used to test these concepts quickly, easily, and economically, while keeping weight and alignment constant. The VSPA Foot naturally takes an anthropomorphic form factor, easily fitting into a shoe. The ankle axis is at a biologically appropriate height, and by integrating the spring and sliding mechanism into the keel, the total height is kept low, making it wearable for amputees with long residual limbs.

VII. Conclusion

In this paper, we described the need and specific requirements for a variable stiffness prosthetic ankle with a nonlinear torque-angle curve, and introduced a design that fulfills this need. The nonlinear torque-angle curve was created with a cam transmission, and the stiffness modulation was enabled by active control of the fiberglass leaf spring's support condition. We characterized the ankle's range of torque-angle curves for a cam profile that was optimized for level ground walking. A unilateral transtibial amputee performed several ambulation tasks on the prosthesis, and this pilot study indicated more normative range of motion on ramps and stairs. Future work will involve a more thorough biomechanical characterization of the effects of stiffness during different mobility tasks, validation

of a paired intent recognition system, and an analysis of the effects of quasi-stiffness shape on metabolic cost of gait.

ACKNOWLEDGMENT

The authors would like to thank Gordon Composites for donating the fiberglass spring. This work made use of the Central Laboratory for Materials Mechanical Properties supported by the MRSEC Program of the National Science Foundation (DMR-1121262) at the Northwestern University Materials Research Science and Engineering Center. This work was performed in the Neurobionics Lab, Center for Bionic Medicine, Shirley Ryan AbilityLab (formerly the Rehabilitation Institute of Chicago).

REFERENCES

[1] K. Ziegler-Graham *et al.*, "Estimating the prevalence of limb loss in the United States: 2005 to 2050," *Arch. Phys. Med. Rehabil.*, vol. 89, no. 3, pp. 422–429, 2008.

[2] G. K. Klute, C. F. Kallfelz, and J. M. Czerniecki, "Mechanical properties of prosthetic limbs: Adapting to the patient," *J. Rehabil. Res. Device*, vol. 38, no. 3, pp. 299–307, 2001.

[3] J. Kulkarni, S. Wright, C. Toole, J. Morris, and R. Hirons, "Falls in patients with lower limb amputations: Prevalence and contributing factors," *Physiotherapy*, vol. 82, no. 2, pp. 130–136, 1996.

[4] R. L. Waters and S. Mulroy, "The energy expenditure of normal and pathologic gait," *Gait Posture*, vol. 9, no. 3, pp. 207–231, 1999.

[5] W. C. Miller, M. Speechley, and B. Deathe, "The prevalence and risk factors of falling and fear of falling among lower extremity amputees," *Arch. Phys. Med. Rehabil.*, vol. 82, no. 8, pp. 1031–1037, 2001.

[6] A. R. De Asha, L. Johnson, R. Munjal, J. Kulkarni, and J. G. Buckley, "Attenuation of centre-of-pressure trajectory fluctuations under the prosthetic foot when using an articulating hydraulic ankle attachment compared to fixed attachment," *Clin. Biomech.*, vol. 28, no. 2, pp. 218–224, 2013.

[7] J. Perry, L. A. Boyd, S. S. Rao, and S. J. Mulroy, "Prosthetic weight acceptance mechanics in transtibial amputees wearing the Single Axis, Seattle Lite, and Flex Foot," *IEEE Trans. Rehabil. Eng.*, vol. 5, no. 4, pp. 283–289, Dec. 1997.

[8] A. H. Hansen and C. C. Wang, "Effective rocker shapes used by able-bodied persons for walking and fore-aft swaying: Implications for design of ankle-foot prostheses," *Gait Posture*, vol. 32, no. 2, pp. 181–184, 2010.

[9] C. M. Powers, L. A. Boyd, L. Torburn, and J. Perry, "Stair ambulation in persons with transtibial amputation: An analysis of the Seattle LightFoot," *J. Rehabil. Res. Device*, vol. 34, pp. 9–18, Jan. 1997.

[10] L. Torburn, G. P. Schweiger, J. Perry, and C. M. Powers, "Below-knee amputee gait in stair ambulation: A comparison of stride characteristics using five different prosthetic feet," *Clin. Orthopaedics Rel. Res.*, vol. 303, pp. 185–192, Jun. 1994.

[11] V. Struchkov and J. G. Buckley, "Biomechanics of ramp descent in unilateral trans-tibial amputees: Comparison of a microprocessor controlled foot with conventional ankle-foot mechanisms," *Clin. Biomech.*, vol. 32, pp. 164–170, Feb. 2016.

[12] M. Alimusaj, L. Fradet, F. Braatz, H. J. Gerner, and S. I. Wolf, "Kinematics and kinetics with an adaptive ankle foot system during stair ambulation of transtibial amputees," *Gait Posture*, vol. 30, no. 3, pp. 356–363, 2009.

[13] L. Fradet, M. Alimusaj, F. Braatz, and S. I. Wolf, "Biomechanical analysis of ramp ambulation of transtibial amputees with an adaptive ankle foot system," *Gait Posture*, vol. 32, no. 2, pp. 191–198, 2010.

[14] M. K. Shepherd and E. J. Rouse, "Design of a quasi-passive ankle-foot prosthesis with biomimetic, variable stiffness," in *Proc. IEEE Int. Conf. Robot. Autom.*, 2017, pp. 6672–6678.

[15] G. Bovi, M. Rabuffetti, P. Mazzoleni, and M. Ferrarin, "A multiple-task gait analysis approach: Kinematic, kinetic and EMG reference data for healthy young and adult subjects," *Gait Posture*, vol. 33, no. 1, pp. 6–13, 2011.

[16] E. J. Rouse, L. J. Hargrove, E. J. Perreault, and T. A. Kuiken, "Estimation of human ankle impedance during the stance phase of walking," *IEEE Trans. Neural Syst. Rehabil. Eng.*, vol. 22, no. 4, pp. 870–878, Jul. 2014.

[17] E. J. Rouse, R. D. Gregg, L. J. Hargrove, and J. W. Sensinger, "The difference between stiffness and quasi-stiffness in the context of biomechanical modeling," *IEEE Trans. Biomed. Eng.*, vol. 60, no. 2, pp. 562–568, Feb. 2013.

[18] M. J. Major, M. Twiste, L. P. Kenney, and D. Howard, "The effects of prosthetic ankle stiffness on stability of gait in people with transtibial amputation," *J. Rehabil. Res. Device*, vol. 53, no. 6, pp. 839–852, 2016.

[19] A. H. Hansen, D. S. Childress, S. C. Miff, S. A. Gard, K. P. Mesplay, "The human ankle during walking: Implications for design of biomimetic ankle prostheses," *J. Biomech.*, vol. 37, no. 10, pp. 1467–1474, 2004.

[20] D. A. Winter, *Biomechanics and Motor Control of Human Movement*, 2nd ed. Hoboken, NJ, USA: Wiley, 2005.

[21] K. Shamaei, G. S. Sawicki, and A. M. Dollar, "Estimation of quasi-stiffness and propulsive work of the human ankle in the stance phase of walking," *PLoS ONE*, vol. 8, no. 3, p. e59935, 2013.

[22] D. R. Vickers, C. Palk, A. S. McIntosh, and K. T. Beatty, "Elderly unilateral transtibial amputee gait on an inclined walkway: A biomechanical analysis," *Gait Posture*, vol. 27, no. 3, pp. 518–529, 2008.

[23] E. Nickel, J. Sensinger, and A. Hansen, "Passive prosthetic ankle-foot mechanism for automatic adaptation to sloped surfaces," *J. Rehabil. Res. Device*, vol. 51, no. 5, pp. 803–814, 2014.

[24] T. T. Sowell, "A preliminary clinical evaluation of the Mauch hydraulic foot-ankle system," *Prosthetics Orthotics Int.*, vol. 5, no. 2, pp. 87–91, 1981.

[25] P. X. Ku, N. A. A. Osman, and W. A. B. W. Abas, "Balance control in lower extremity amputees during quiet standing: A systematic review," *Gait Posture*, vol. 39, no. 2, pp. 672–682, 2014.

[26] P. G. Morasso and M. Schieppati, "Can muscle stiffness alone stabilize upright standing?" *J. Neurophysiol.*, vol. 82, pp. 1622–1626, Sep. 1999.

[27] J. M. Caputo and S. H. Collins, "A universal ankle-foot prosthesis emulator for human locomotion experiments," *J. Biomech. Eng.*, vol. 136, no. 3, p. 35002, 2014.

[28] J. J. Gorges, *Controlled Coronal Stiffness Prosthetic Ankle for Improving Balance on Uneven Terrain*. Seattle, WA, USA: Univ. Washington, 2013.

[29] B. Vanderborght *et al.*, "Variable impedance actuators: A review," *Robot. Auto. Syst.*, vol. 61, no. 12, pp. 1601–1614, 2013.

[30] L. L. Howell, *Compliant Mechanisms*. Hoboken, NJ, USA: Wiley, 2001.

[31] J. Realmuto, G. Klute, and S. Devasia, "Nonlinear passive cam-based springs for powered ankle prostheses," *J. Med. Device*, vol. 9, no. 1, p. 011007, 2014.

[32] A. S. McIntosh, K. T. Beatty, L. N. Dwan, and D. R. Vickers, "Gait dynamics on an inclined walkway," *J. Biomech.*, vol. 39, no. 13, pp. 2491–2502, 2006.

[33] K. E. Zelik *et al.*, "Systematic variation of prosthetic foot spring affects center-of-mass mechanics and metabolic cost during walking," *IEEE Trans. Neural Syst. Rehabil. Eng.*, vol. 19, no. 4, pp. 411–419, Apr. 2011.

[34] A. M. Simon *et al.*, "Delaying ambulation mode transition decisions improves accuracy of a flexible control system for powered knee-ankle prosthesis," *IEEE Trans. Neural Syst. Rehabil. Eng.*, vol. 25, no. 8, pp. 1164–1171, Aug. 2016.

[35] R. E. Quesada, J. M. Caputo, and S. H. Collins, "Increasing ankle push-off work with a powered prosthesis does not necessarily reduce metabolic rate for transtibial amputees," *J. Biomech.*, vol. 49, no. 14, pp. 3452–3459, 2016.

[36] E. S. Gardinier *et al.*, "A controlled clinical trial of a clinically-tuned powered ankle prosthesis in people with transtibial amputation," *Clin. Rehabil.*, 2017.

[37] D. H. Gates, J. M. Aldridge, and J. M. Wilken, "Kinematic comparison of walking on uneven ground using powered and unpowered prostheses," *Clin. Biomech.*, vol. 28, no. 4, pp. 467–472, 2013.

[38] P.-F. Su *et al.*, "The effects of increased prosthetic ankle motions on the gait of persons with bilateral transtibial amputations," *Amer. J. Phys. Med. Rehabil.*, vol. 89, no. 1, pp. 34–47, 2010.

[39] Y. Hermodsson *et al.*, "Standing balance in trans-tibial amputees following vascular disease or trauma: A comparative study with healthy subjects," *Prosthet. Orthot. Int.*, vol. 18, no. 3, pp. 150–158, 1994.

[40] T. M. Quai, S. G. Brauer, and J. C. Nitz, "Somatosensation, circulation and stance balance in elderly dysvascular transtibial amputees," *Clin. Rehabil.*, vol. 19, no. 6, pp. 668–676, 2005.

[41] M. Seth and E. Lamberg, "Standing balance in people with trans-tibial amputation due to vascular causes: A literature review," *Prosthetics Orthotics Int.*, vol. 41, no. 4, pp. 345–355, 2017.

[42] A. Protopapadaki, W. I. Drechsler, M. C. Cramp, F. J. Coutts, and O. M. Scott, "Hip, knee, ankle kinematics and kinetics during stair ascent and descent in healthy young individuals," *Clin. Biomech.*, vol. 22, no. 2, pp. 203–210, 2006.

Max K. Shepherd (S'14) received the B.S. degree with the Department of Biomedical Engineering, University of North Carolina, Chapel Hill, in 2012. He is currently pursuing the Ph.D. degree in biomedical engineering with Northwestern University, Evanston. He was a recipient of the American Heart Association Pre-Doctoral Fellowship.

From 2012 to 2014, he was an Intern with the Institute for Human and Machine Cognition, Walt Disney Imagineering, and the Robotics and Mechanisms Lab, Virginia Tech. His research interests include gait biomechanics, stroke rehabilitation, and the design and control of prosthetics and exoskeletons.

Elliott J. Rouse (S'10–M'12) received the B.S. degree in mechanical engineering from The Ohio State University, Columbus, OH, USA, in 2007, the M.S. and Ph.D. degrees in biomedical engineering from Northwestern University, Evanston, IL, USA, in 2009 and 2012. Subsequently, he joined the Massachusetts Institute of Technology, Cambridge, MA, USA, where he was a Post-Doctoral Fellow with the Biomechatronics Group, MIT Media Lab, until 2014.

He is currently an Assistant Professor with the Department of Mechanical Engineering, University of Michigan, where he directs the Neurobionics Lab, Ann Arbor, MI, USA. His current research focuses on understanding locomotion using techniques from system dynamics and robotics, and how pathology affects these dynamics. The goal of this understanding is to develop a new class of wearable robotic technologies that impact the lives of people with disabilities. Applications include robotic prostheses, exoskeletons, and technologies that augment human motor performance. He serves on the IEEE Technical Committee on Bio-robotics, and the Editorial Board for the *Journal Assistive Technology*.